Supplementary Information

Bright CuInS$_2$/CdS Nanocrystal Phosphors for High-Gain Full-Spectrum Luminescent Solar Concentrators

Kathryn E. Knowles,[a] Troy B. Kilburn,[a] Dane G. Alzate,[a] Stephen McDowall,[b]
and Daniel R. Gamelin[a],*

[a]*Department of Chemistry, University of Washington, Seattle, Washington 98195-1700, United States,* [b]*Mathematics Department, Western Washington University, 516 High Street, Bellingham, Washington 98225, United States*

e-mail: gamelin@chem.washington.edu

EXPERIMENTAL METHODS

Synthesis of CuInS$_2$/CdS NCs. Indium(III) acetate, copper(I) iodide, cadmium nitrate tetrahydrate, myristic acid, sulfur, 1-dodecanethiol, and 1-octadecene were purchased from Sigma Aldrich; n-trioctylphosphine was purchased from Strem; and potassium hydroxide was purchased from EMD. All reagents were used without further purification.

We followed a literature procedure,[1] with minor modifications, to make CuInS$_2$/CdS core/shell NCs. To make the CuInS$_2$ core nanocrystals, we degassed a mixture of 0.293 g indium acetate, 0.189 g of copper(I) iodide, and 5 mL 1-dodecanethiol in a 50 mL three neck round bottom flask at room temperature with three cycles of pulling vacuum for 5 minutes followed by purging with nitrogen. After the final nitrogen purge, the reaction was heated to 100 ˚C for 10 minutes and the solution gradually turned yellow. We heated the reaction at 230 ˚C for 10 minutes, then cooled it rapidly to 60 ˚C.

To grow CdS shells, we first prepared cadmium myristate by dripping 5 mL of a 0.2 M solution of cadmium nitrate in anhydrous methanol into 30 mL of a 0.1 M solution of myristic acid in anhydrous ethanol. The resulting white precipitate was collected and dried. We then prepared a solution of shell growth precursors by heating and sonicating 0.225 g cadmium myristate, 0.014 g sulfur, 4 mL 1-octadecene, and 0.4 mL n-trioctylphosphine to form a uniform white dispersion. The shell growth precursors were injected into a solution containing 1.0 mL of crude CuInS$_2$ reaction solution and 4.0 mL 1-octadecene at 210 ˚C at a rate of 0.2 mL/min. After addition of the shell growth precursors was complete, the reaction was cooled to 60 ˚C gradually, 1 mL oleic acid and 1 mL toluene were added, and the mixture was stirred for 10 minutes. The resulting CuInS$_2$/CdS core/shell nanocrystals were purified with several cycles of precipitation upon addition of ethanol followed by resuspension in toluene.

Inductively Coupled Plasma Atomic Emission Spectroscopy. We digested dried pellets of CuInS$_2$ and CuInS$_2$/CdS core/shell NCs in 0.2 mL of concentrated ultrapure nitric acid. The digested samples were then diluted to 10 mL with ultrapure water and passed through 0.2 μm cellulose acetate syringe filters before the concentrations of Cu, In and Cd were measured on a Perkin-Elmer 8300 inductively coupled plasma atomic emission spectrometer. We generated

calibration curves for the Cu, In, and Cd atomic emission peaks using a series of solutions with known Cu, In, and Cd concentrations prepared by diluting purchased standards (1000 mg/L, High Purity Standards). Using this method, we obtained Cu:In:Cd ratios of 1:1.12:0 and 1:1.06:1.23 for $CuInS_2$ and $CuInS_2$/CdS NCs, respectively.

Spectroscopic Methods. Absorption and PL spectra were taken on a Cary 5000 spectrometer and an Ocean Optics USB-2000+ spectrometer corrected for spectral sensitivity, respectively. We used a Hamamatsu integrating sphere quantum yield measurement system with 500-nm excitation to measure the photoluminescence quantum yield of tetrachloroethylene solutions of $CuInS_2$/CdS NCs in a 1-cm pathlength cuvette. The accuracy of this apparatus was confirmed through measurement of a known quantum yield standard. We took several quantum yield measurements of $CuInS_2$/CdS NC solutions with different concentrations to identify a range where reabsorption effects are negligible, and in this range the measured quantum yield is independent of concentration. At least three measurements were made at each concentration to account for inherent uncertainties in the measurement due to, for example, minor fluctuations in the intensity of the excitation source. The details of the 1D LSC liquid waveguide apparatus were reported previously.[2] Data collected from a 100-fold diluted solution of $CuInS_2$/CdS NCs in tetrachloroethylene ($OD_t = 0.01$) were used to correct for scattering losses due to imperfections in the waveguide.

Powder X-ray Diffraction.
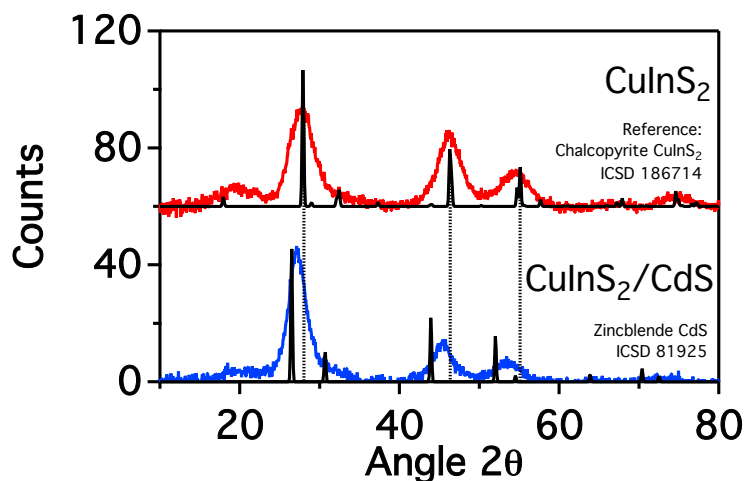
Figure S1. Powder x-ray diffraction patterns of films of $CuInS_2$ cores and $CuInS_2$/CdS core/shell NCs dropcast onto silicon wafers obtained on a Bruker D8 Discover spectrometer at the University of Washington Nanotech User Facility. These spectra indicate that both $CuInS_2$ cores and $CuInS_2$/CdS core/shell NCs have the chalcopyrite crystal structure. Analysis of the linewidths of these spectra using the Scherrer-Debye equation indicates average crystalline domain sizes of 2.6 and 3.4 nm for the $CuInS_2$ cores and $CuInS_2$/CdS core/shell NCs, respectively.

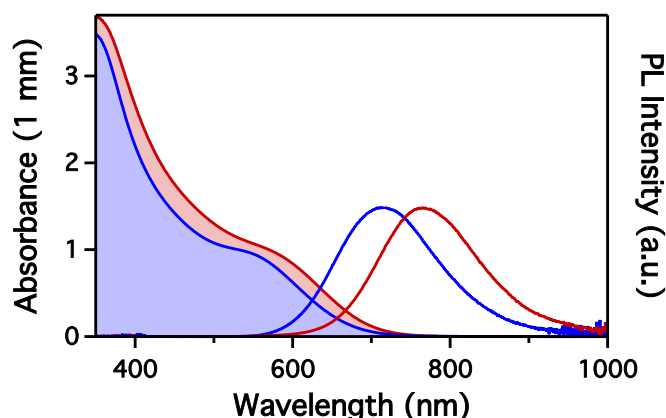**Absorption and PL Spectra of CuInS$_2$ and CuInS$_2$/CdS Core/Shell Nanocrystals.**
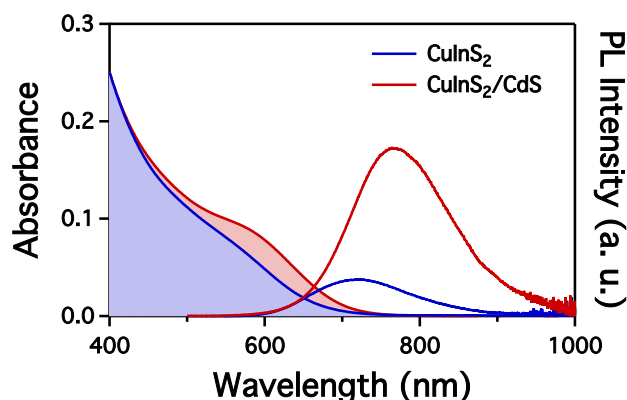
Figure S2. Absorption (solid lines with shading) and PL spectra of toluene solutions of CuInS$_2$ core (blue) and CuInS$_2$/CdS core/shell (red) nanocrystals that have the same optical density at the PL excitation wavelength (405 nm). Upon growth of the CdS shell, the absorption and PL spectra both shift to lower energy, and the PL quantum yield increases from ~0.15 to 0.86 ± 0.02.

**Transmission Electron Microscopy (TEM) of CuInS$_2$/CdS NCs.**
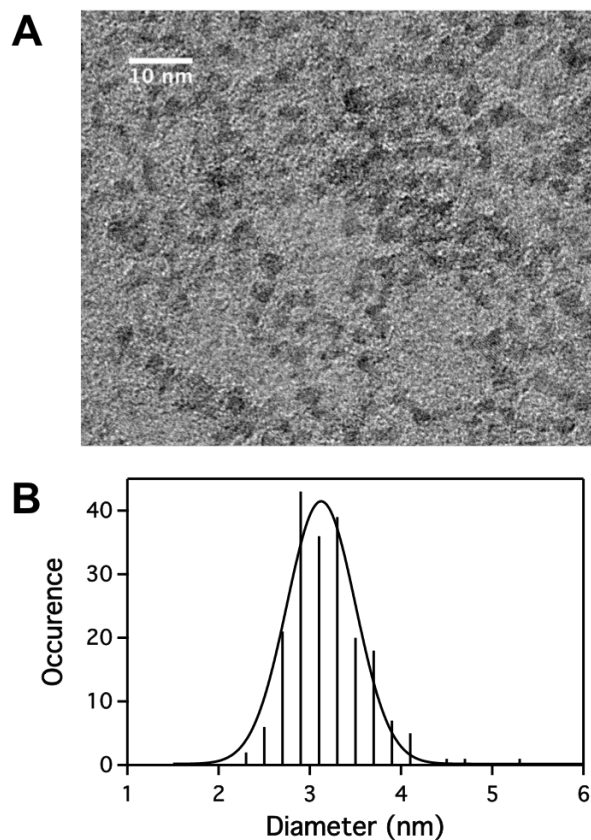
Figure S3. A Representative TEM image of CuInS$_2$/CdS nanocrystals collected on an FEI tecnai microscope. **B** Histogram containing measured diameters of 200 nanocrystals and fit to a Gaussian distribution with an average and standard deviation of 3.1 ± 0.5 nm.

**CuInS₂/CdS NCs with larger band gaps have smaller solar absorption.**

Figure S4. Absorption (solid lines with shading) and PL spectra of two different samples CuInS₂/CdS core/shell nanocrystals dispersed in tetrachloroethylene. The absorption spectra were collected over a 1 mm pathlength. The samples have nearly identical quantum yields, ($\eta_{PL,blue}$ = 0.87 ± 0.02, $\eta_{PL,red}$ = 0.86 ± 0.02), but they have different solar absorptions ($A_{sol,NC}$). The sample represented by the blue spectra has $A_{sol,NC}$ = 8.3 × 10^{20} photons/m²s and the sample represented by the red spectra has $A_{sol,NC}$ = 9.2 × 10^{20} photons/m²s. The spectra for the sample used as an LSC phosphor in the main text are plotted in red.

**CuInS₂/CdS NCs have the Lowest Probability of Reabsorption at Long Reduced Pathlengths.**
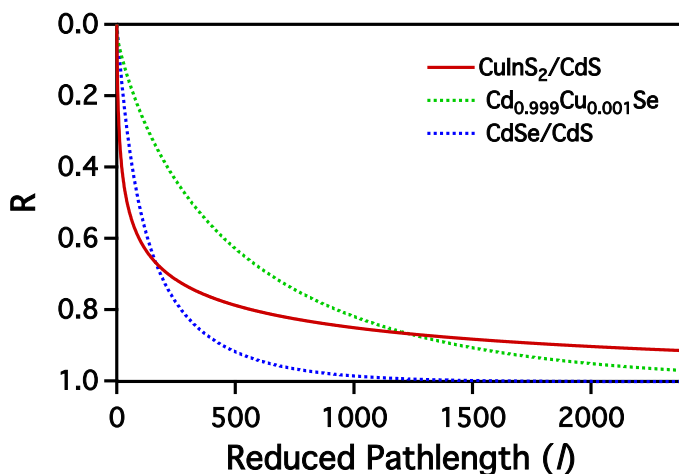
Figure S5. Probability of reabsorption, *R*, calculated from eq. 1 in the main text and plotted versus reduced pathlength, *l*, out to *l* = 2400 for CuInS₂/CdS (solid red line), Cd₀.₉₉₉Cu₀.₀₀₁Se (dashed green line) and CdSe/CdS core/shell (dashed blue line) NCs. The data for CuInS₂/CdS were calculated using the spectra shown in Figure 1A in the main text, and the data for Cd₀.₉₉₉Cu₀.₀₀₁Se and CdSe/CdS were calculated from spectra previously reported in ref. 2.

Correcting data collected from the 1D LSC for waveguide losses does not affect the qualitative results.
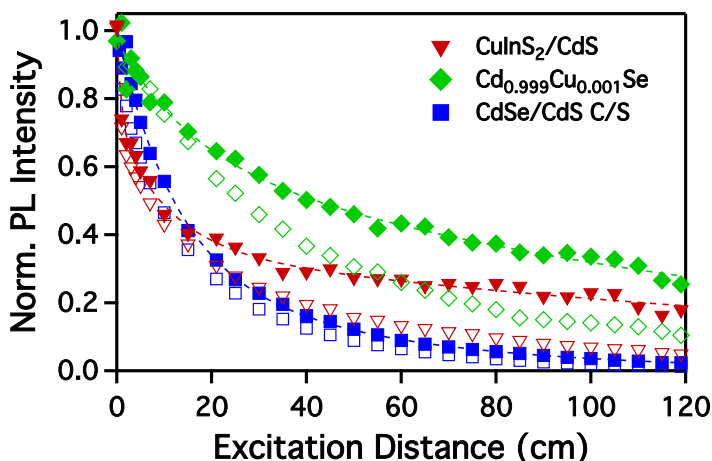
Figure S6. Plot of integrated PL intensity measured in the 1D LSC versus excitation distance, L, normalized at $L = 0$. Open symbols represent raw data and closed symbols represent data corrected for losses due to imperfections in the 1D LSC waveguide. Data collected for 100-fold diluted solutions ($OD_t = 0.01$) of each sample were used to generate the waveguide correction curves. Data for $Cd_{0.999}Cu_{0.001}Se$ and CdSe/CdS NCs are from ref. 2.

The projected 2D flux gain for a square LSC containing CuInS$_2$/CdS NCs does not reach a maximum value even for unrealistically large side lengths.
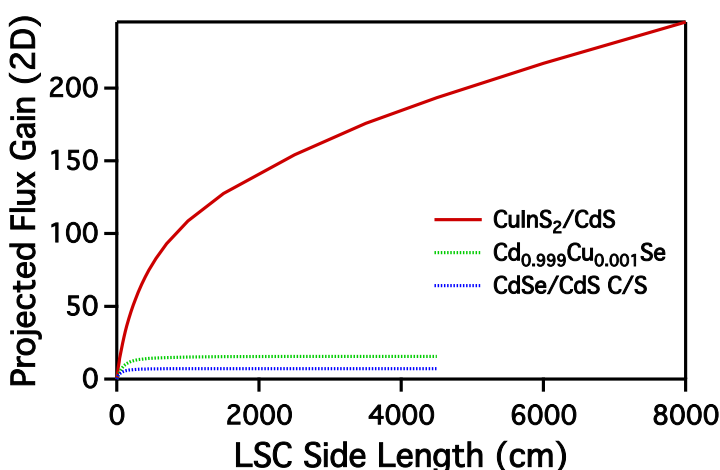
Figure S7. Projected flux gains of square 2D LSCs containing CuInS$_2$/CdS (solid red line), $Cd_{0.999}Cu_{0.001}Se$ (dashed green line), or CdSe/CdS (dashed blue line) NCs and coupled to Si PVs on all four edges under AM 1.5 solar irradiation plotted versus LSC side length. Data for $Cd_{0.999}Cu_{0.001}Se$ and CdSe/CdS NCs are from ref. 2. The x axis

shows projections out to unrealistically large length scales to illustrate the absence of a maximum in the $CuInS_2/CdS$ curve.

References

1   L. Li, A. Pandey, D. J. Werder, B. P. Khanal, J. M. Pietryga and V. I. Klimov, *J. Am. Chem. Soc.,* 2011, **133**, 1176.

2   L. R. Bradshaw, K. E. Knowles, S. McDowall and D. R. Gamelin, *Nano Lett.,* 2015, **15**, 1315.